

# Compression and Reflection of Visually Evoked Cortical Waves

Weifeng Xu,<sup>1</sup> Xiaoying Huang,<sup>1</sup> Kentaroh Takagaki,<sup>1</sup> and Jian-young Wu<sup>1,\*</sup>

<sup>1</sup>Department of Physiology and Biophysics, Georgetown University Medical Center, Washington, DC 20057, USA

\*Correspondence: wuj@georgetown.edu

DOI 10.1016/j.neuron.2007.06.016

## SUMMARY

Neuronal interactions between primary and secondary visual cortical areas are important for visual processing, but the spatiotemporal patterns of the interaction are not well understood. We used voltage-sensitive dye imaging to visualize neuronal activity in rat visual cortex and found visually evoked waves propagating from V1 to other visual areas. A primary wave originated in the monocular area of V1 and was “compressed” when propagating to V2. A reflected wave initiated after compression and propagated backward into V1. The compression occurred at the V1/V2 border, and local GABA<sub>A</sub> inhibition is important for the compression. The compression/reflection pattern provides a two-phase modulation: V1 is first depolarized by the primary wave, and then V1 and V2 are simultaneously depolarized by the reflected and primary waves, respectively. The compression/reflection pattern only occurred for evoked waves and not for spontaneous waves, suggesting that it is organized by an internal mechanism associated with visual processing.

## INTRODUCTION

During visual processing, extensive interactions occur both within the primary visual cortex (V1) and between visual areas via feedforward and feedback projections (Rockland and Pandya, 1981; Kennedy and Bullier, 1985; Livingstone and Hubel, 1987, 1988; Angelucci et al., 2002; Sincich and Horton, 2002a, 2002b, 2003; Shmuel et al., 2005). Such intra- and interareal interactions may follow a stereotypical spatial pattern and temporal sequence between the visual areas, and may manifest as propagation of excitation waves at the population level. In invertebrates and lower vertebrates, propagating waves have been suggested to participate in visual and olfactory processing (Delaney et al., 1994; Precht et al., 1997, 2000; Senseman and Robbins, 1999; Lam et al., 2000, 2003). In mammals, propagating waves have also been observed in somatosensory cortex and olfactory

bulb (Freeman and Barrie, 2000; Derdikman et al., 2003; Petersen et al., 2003a, 2003b; Civillico and Contreras, 2006; Ferezou et al., 2006). In motor cortex, waves have been suggested to mediate information transfer during movement preparation and execution (Rubino et al., 2006). However, in mammalian visual cortex, while waves have been reported in a few studies (Arieli et al., 1995; Roland et al., 2006), the spatiotemporal patterns of evoked waves have not been carefully examined. Since propagating waves determine when and where population depolarization will occur in the cortical network, they may play critical roles in cortical processing (Ermentrout and Kleinfeld, 2001; Rubino et al., 2006). Thus, characterizing the initiation and spatiotemporal patterns of the evoked waves in visual areas is important for understanding the population mechanisms of visual processing.

Voltage-sensitive dye (VSD) imaging provides a useful tool for visualizing the spatiotemporal patterns of cortical activity. With the improvement of blue dyes (Shoham et al., 1999), sensory-evoked activity from mammalian cortex can be observed in vivo with high signal-to-noise ratio (Derdikman et al., 2003; Petersen et al., 2003a, 2003b; Grinvald and Hildesheim, 2004; Ferezou et al., 2006; Chen et al., 2006). In this study, we used VSD imaging to examine visually evoked activity in rat visual cortical areas. Our imaging device offers 17–19 bit dynamic range, allowing us to examine wave dynamics in detail in single trials (Lippert et al., 2007). We found that a visual stimulus initiated a propagating wave in V1, which was compressed when propagating to V2. A reflected wave was subsequently initiated and propagated back into V1. Further study showed that the compression occurred at the V1/V2 border. Similar compression/reflection patterns were also observed at the border between mediomedial V2 (V2MM) and retrosplenial dysgranular (RSD) areas. These compression/reflection patterns occur only in evoked waves and not in spontaneous waves, suggesting that the compression and reflection are governed by mechanisms specific for processing visual inputs.

## RESULTS

### Evoked Waves: Compression and Reflection

VSD signals were measured from V1 and V2 areas of anesthetized rat with a photodiode array (Figure 1A). The visual stimulus was a drifting grating (0.05 cycles/degree,

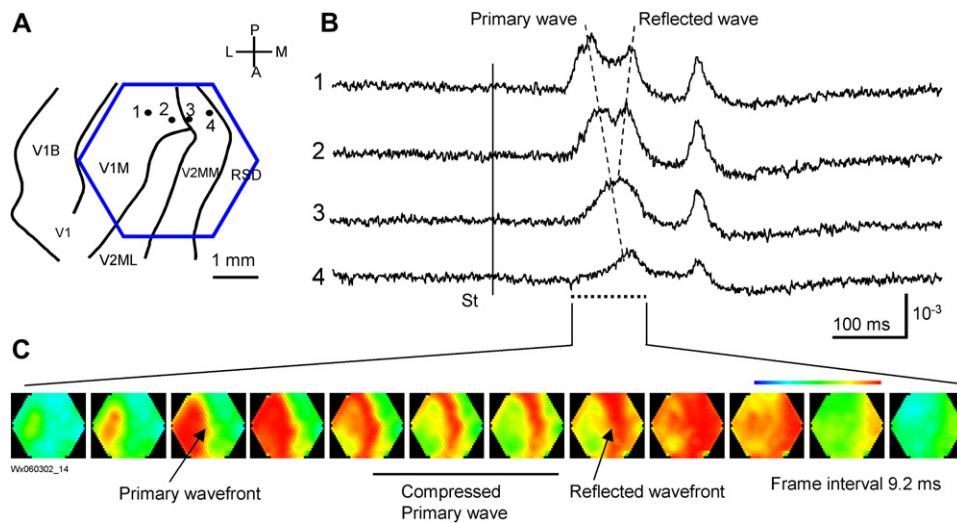


**Figure 1. Wave Compression and Reflection**

(A) Schematic drawing of imaging field (blue hexagon) overlying the map of the visual areas (left hemisphere; the map is shown as a mirror image of the cortex due to conversion in the microscope). Four optical detectors, 1–4, were selected (out of a total of 464 detectors) and their signal traces are shown on the right (B). V1B, V1M: binocular and monocular areas of V1, respectively; V2MM, V2ML: mediomedial and mediolateral areas of V2, respectively; RSD: retrosplenial dysgranular. The map shown was made according to the stereotaxic map of Paxinos and Watson (2005). (B) Optical signals of visually evoked activity from four detectors (1–4). A grating (0.05 cycles/degree,  $50^{\circ} \times 38^{\circ}$  degrees of viewing angle) was constantly presented to the contralateral eye. Drifting of the grating (3 cycles/s) was used as visual stimulus, with onset time marked by the vertical line (St). The peak of the activity occurred sequentially from detector 1 to 4, indicating a forward-propagating wave (primary wave) from V1 to V2 (left broken line). A reflected wave can be seen starting from detector 3 and propagating backward to detector 1 (right broken line). The two waves can be clearly seen in the bottom images. (C) The pseudocolor images (0.6 ms snapshots) of the initial section of the evoked response. Twelve images (time marked by the dotted line under the traces) are shown from a total of 8192 frames in a 5 s recording trial. On each detector, the amplitude of the signal was converted to pseudocolor according to a linear color scale (peak, red; baseline, blue). The first image was taken when the evoked primary wave first appeared in the V1M, approximately 104 ms after the grating started to drift.

$50^{\circ} \times 38^{\circ}$  degrees of viewing angle) presented to the contralateral eye. The drift of the grating (3 cycles/s) reliably evoked a propagating wave in the visual cortex. The evoked wave initiated with a latency of  $\sim 100$  ms ( $99.8 \pm 18.2$  ms, mean  $\pm$  standard deviation [SD],  $n = 115$  trials) after the onset of the drifting, and the activity was seen in all optical detectors, with a small time difference between each detector (Figure 1B, traces 1–4). The signal on each individual detector was converted to pseudocolor according to a linear color scale. The pseudocolor images showed that the evoked wave initiated in the monocular area of V1 (V1M) and propagated in both directions to the V1 binocular area (V1B) and to V2. This evoked wave, referred to as the primary wave, was “compressed” in its spatial dimension into a thin band in the middle of the propagating path (Figure 1C). A reflected wave initiated after compression and propagated backward to V1 (Figure 1C). The primary and reflected waves can be identified in the signal traces of individual detectors as double peaks (Figure 1B). Supplemental Movie S1, in the Supplemental Data available with this article online, presents another example showing the spatiotemporal sequence of the compression/reflection.

This compression/reflection pattern was reliably observed in different recording trials. Figure 2A shows wave patterns from the same animal produced with iden-

tical stimuli (intertrial interval of  $\sim 200$  s). In this animal, the compression bands reached the narrowest width (Figure 2A, column c) at  $72.7 \pm 7.2$  ms (mean  $\pm$  SD,  $n = 9$ ) after the onset of the primary wave. The compression band then became wider again due to the wave propagating into V2 and the back propagation of the reflected wave (Figure 2A, column d). The location and the shape of the compression band were similar from trial to trial. Movie S2 provides an example from another animal, in which three trials show almost identical location and temporal sequence for the wave compression. We have examined the visually evoked waves in 36 animals, and a similar primary wave, compression band, and reflected wave were observed in all animals. In Figure 2B, representative trials from seven animals all show similar spatiotemporal patterns. In different animals, the locations of the compression and the shape of the compression band varied slightly, probably reflecting individual variability in the neuroanatomy of the visual areas.

A similar compression/reflection pattern was observed under visual stimuli with various parameters, including alternation of orientation ( $0^{\circ}$ ,  $90^{\circ}$ ,  $180^{\circ}$ , or  $270^{\circ}$ ), drifting velocity (30–200 degree/s), spatial frequency (0.025–0.3 cycles/degree), stimulus position (Figure S3 in the Supplemental Data available with this article online), contrast ( $>0.5$ , Figure S4) and size ( $>10^{\circ}$ , Figure S4), while the

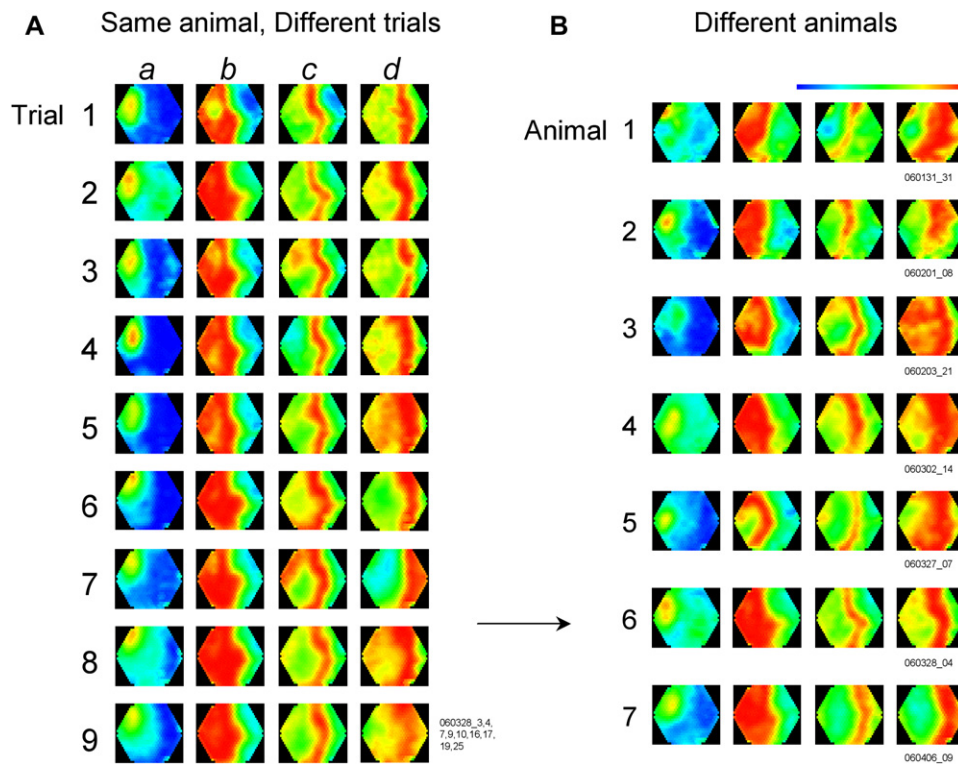


**Figure 2. Wave Compression Occurs Robustly**

(A) Nine recording trials from one animal. In each trial four images are chosen from four stages of the evoked wave: *a*, initiation of the primary wave; *b*, full expansion of the primary wave in V1 and the start of the compression; *c*, full compression (band at narrowest); and *d*, after the compression, in which the waves move forward into V2 and reflect backward into V1. The evoked wave patterns were stable over a period of  $\sim 2$  hr.

(B) Evoked waves from seven animals (1–7) showing similar compression patterns. The animal in (A) is shown as animal 6 in (B).

Color scale bar: the amplitude of the signal from each detector was converted to pseudo-color according to a linear color scale; red represents the peak and blue represents the baseline.

probability for initiating the primary wave, the initiation site, and the shape of the compression band could be altered by varying stimulus parameters. Changes in stimulus position altered the location of the primary wave initiation site, consistent with the retinotopic map in V1M (Figures S2 and S3A). The shape of the compression band also varied when the location of the initiation site changed (red and blue lines in Figure S3A). The probability of evoking the wave decreased when either stimulus size or contrast was reduced, with a threshold of  $6^\circ$ – $10^\circ$  and  $0.2^\circ$ – $0.5^\circ$ , respectively (Figure S4). However, once the primary wave was initiated by suprathreshold stimulation, the same pattern of compression/reflection occurred. This was true even when the stimulus was presented at two positions with a large difference in the visual field (Figure S3B, top and middle row). Thus, the wave compression/reflection pattern is the rule rather than the exception.

#### Compression at the Border between Visual Areas?

The reliability of the wave compression suggests it may be related to the neuroanatomical structure of the cortex, especially the border between V1 and V2. To test this idea, we used corpus callosum fiber bundles to identify the

V1/V2 border. In rats, these bundles are abundant near the V1/V2 border (Olavarria and Hiroi, 2003), so when electrical shocks were applied to the visual cortex contralateral to the imaging side, action potentials may reach the imaging side by the callosal fibers and be visualized with VSD imaging. Indeed, electrical stimulation of a moderate intensity in the contralateral V1M area evoked a localized activity on the imaging side (Figure 3B). The activity loci on the imaged side were fixed when the stimulation site was fixed, and the poststimulus latency of the activity was short and fixed ( $22.4 \pm 2.6$  ms, mean  $\pm$  SD,  $n = 12$  trials from three animals), indicating that electrical shock evoked the activity on the imaging side via callosal fiber bundles. In the same animal, visually evoked waves (Figure 3A) compressed adjacent to the activity evoked by contralateral electrical shocks (Figures 3C and 3D), suggesting that the compression occurred near the V1/V2 border.

We next examined if compression occurs at borders between other visual areas. Indeed, a second compression often occurred (observed in 11 out of 36 animals) along the propagating path (Figure 4A). The location of the second compression (Figure 4C) was more medial to that of

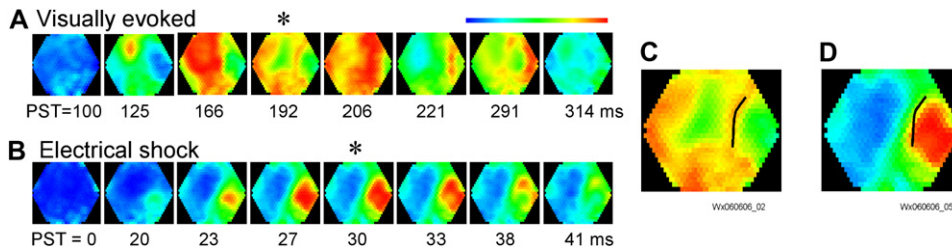


**Figure 3. Compression Band and the Corpus Callosum Fibers**

(A) The visually evoked wave started in V1 (second image) and compressed into a thin band (fourth image). The number below each image indicates the poststimulus time (in ms) for that frame.  
 (B) Images from the same field of view, with activity evoked by an electrical shock to V1M of the contralateral cortex. The activity first appeared at the location of a bundle of afferent callosal fibers. The intensity of the electrical stimulation was small so that the activity in the imaging side was localized without propagation; increasing the stimulus intensity could cause the activity to expand and blur the initiation site.  
 (C and D) The location of the compression band (the center of the band is marked by a black line) is shown adjacent to the activity of the callosal bundle (D). The two images are enlarged from the images in (A) and (B) marked by an asterisk. The black line in (C) is redrawn on (D).  
 Color scale bar: the amplitude of the signal from each detector was converted to pseudo-color according to a linear color scale; red represents the peak and blue represents the baseline.

the first compression (Figure 4B), and probably at the border between V2MM and RSD areas. Between the two compressions there was a narrow gap, which correlated well with the V2MM area (Figure 4C). While the onset time of the second compression was more variable from trial to trial, the location of the second compression was fixed. Multiple compressions suggest that wave compression is associated with the border between visual cortical areas.

**Mechanisms of Wave Compression**

The compression of the primary wave started as an abrupt slowing of the wave leading edge. As shown in Figure 5, the primary wave was initiated by the visual stimulus and quickly expanded into the entire V1 area (Figure 5A, first two images) at a propagation velocity of 50–70 mm/s. When reaching the V1/V2 border, the leading edge of the wavefront had an abrupt slowing (the velocity around the V1/V2 border was about 5 mm/s). Meanwhile, the trailing edge of the wave was still in V1 and maintained a higher speed (50–70 mm/s). As a result, a thin band of compressed activity formed along the V1/V2 border

(Figure 5B). The compression and the resulting thin band sustained for a relatively long time compared with the time taken for the initial propagation within V1. In order to analyze the abrupt slowing of the wave, we present the data in another form of pseudocolor map, the X-T map (Figure 5C), in which the signal on a row of detectors along the propagating direction is displayed against time. In the X-T map the slope of the leading edge is proportional to the propagating velocity, and slowing of the wavefront can be identified as a reduction in the slope. Wave compression can be clearly seen as a thin horizontal stripe at the V1/V2 border (Figure 5C), indicating a nearly zero propagating velocity for about 35 ms during the course of the wave compression.

We assumed that inhibition in local circuits may play a role in the control of velocity. To test if wave compression can be modulated by GABA<sub>A</sub> inhibition, we applied bicuculline, a GABA<sub>A</sub> receptor antagonist, to the cortex. The bicuculline was applied epidurally with a low concentration of 3–5 μM, which is below the threshold of interictal-like spikes (5–10 μM). At low concentration, bicuculline can completely abolish the wave compression without

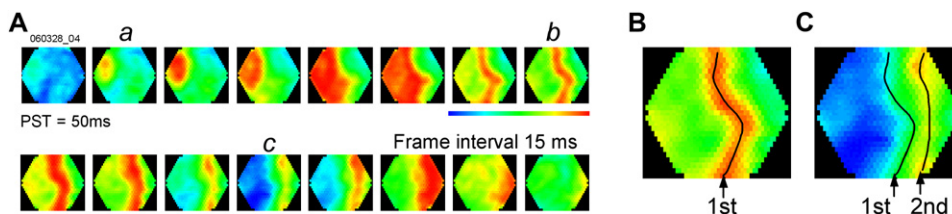


**Figure 4. Multiple Compressions along the Propagating Path**

(A) Sequential snapshots (bottom row follows the top row; interframe interval, 15 ms) during an evoked wave. The wave was initiated in the V1 area (a) and compressed into a thin band at the V1M/V2 border (b). After the compression the wave continued to propagate into the V2 area (bottom row) and compressed again at the V2/RSD border (c).  
 (B and C) Enlarged images of b and c from (A), showing the locations of compression bands.  
 Color scale bar: the amplitude of the signal from each detector was converted to pseudo-color according to a linear color scale; red represents the peak and blue represents the baseline.

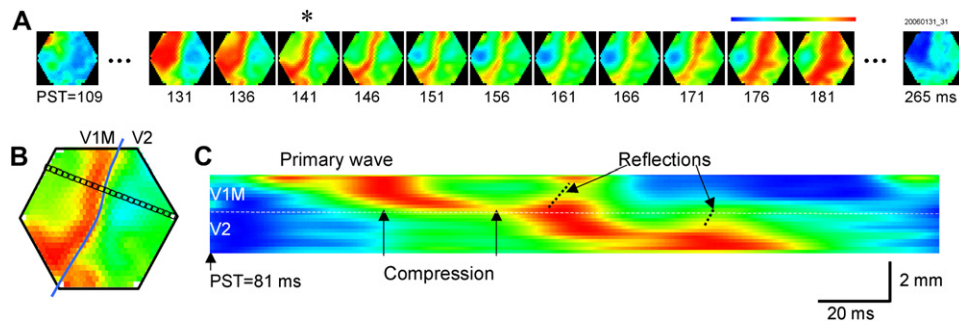


**Figure 5. Velocity Change during Wave Compression**

(A) Selected images (0.6 ms snapshots) of an evoked wave. The number below each image indicates the poststimulus time (in ms) for that frame. The wave initiated at 109 ms poststimulus time (PST, first image) and the compression sustained for  $\sim 35$  ms (136–171 ms). (B) Enlarged frame at 141 ms PST (image in [A] marked with asterisk) overlaid with an anatomy map of V1/V2 border. A row of detectors, starting from the initiation site of the evoked wave and perpendicular to the V1/V2 border, is selected (boxes) for making X-T maps in (C). (C) X-T map made from signals picked up by the row of detectors (boxes in B) showing the space-time of the activity across the V1/V2 border (white dashed line). The thin stripe at the V1/V2 border indicates that compression sustained for a long period. *Movie S1* shows the propagation pattern of this data set.

Color scale bar: the amplitude of the signal from each detector was converted to pseudo-color according to a linear color scale; red represents the peak and blue represents the baseline.

significantly changing the speed of wave propagation within V1 (Figure 6), suggesting that inhibition in the local circuit plays a major role in the wave compression. Compression bands reappeared after bicuculline was washed out (data not shown), suggesting that elimination of the compression band does not require a permanent change in the cortical circuit. Under low dose of bicuculline perfusion, the propagating velocity across the V1/V2 border was the same as that within V1 and V2 (Figure 6B), suggesting that changes in the excitatory connections at the border do not play a major role in the compression.

#### Origin of the Reflected Wave

Reflected waves, while more variable, were observed in most trials (86%, 168/194) following the compression, and they originated near the compression band (Figure 1 and Figure 5C). Since corpus callosum afferent fiber bundles are concentrated near the borders between visual areas, we wanted to determine if the reflected waves were initiated via the callosal fibers by the activity on the

contralateral side of the cortex. Locally applied lidocaine or CNQX to the contralateral cortex significantly suppressed the local EEG response on the contralateral cortex, but it did not block the reflected wave (Figure S5), suggesting that the input from contralateral cortex is not a major contributor to the reflected wave. Thus, the reflected waves are likely to originate ipsilaterally; they may be feedback waves from higher visual areas.

#### Evoked Waves versus Spontaneous Waves

Both evoked and spontaneous cortical activities manifested as propagating waves. The spontaneous activities have also been referred to as “UP states” (Petersen et al., 2003b). It is difficult to distinguish evoked events from spontaneous events in a recording from a single site. However, the spatiotemporal pattern of these two types of events differed markedly. Figure 7 shows wave patterns of two evoked events and six spontaneous events from the same animal. The evoked waves were initiated in V1, compressed near the V1/V2 border, and had

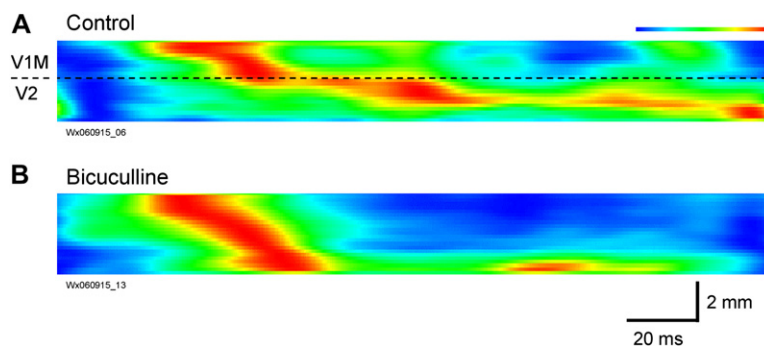


**Figure 6. Bicuculline Eliminates the Wave Compression**

X-T maps from the same field of view, before and after bicuculline treatment.

(A) Under control conditions.

(B) Five micromolar bicuculline was added to the epidural surface. Note: subthreshold concentrations (3–5  $\mu\text{M}$ ) were used to block the GABA<sub>A</sub> receptors. Bicuculline will cause spontaneous interictal-like spikes with a threshold concentration of 5–10  $\mu\text{M}$  (applied epidurally). If spontaneous interictal-like spikes occurred, the animal was excluded from the data set.

Color scale bar: the amplitude of the signal from each detector was converted to pseudo-color according to a linear color scale; red represents the peak and blue represents the baseline.

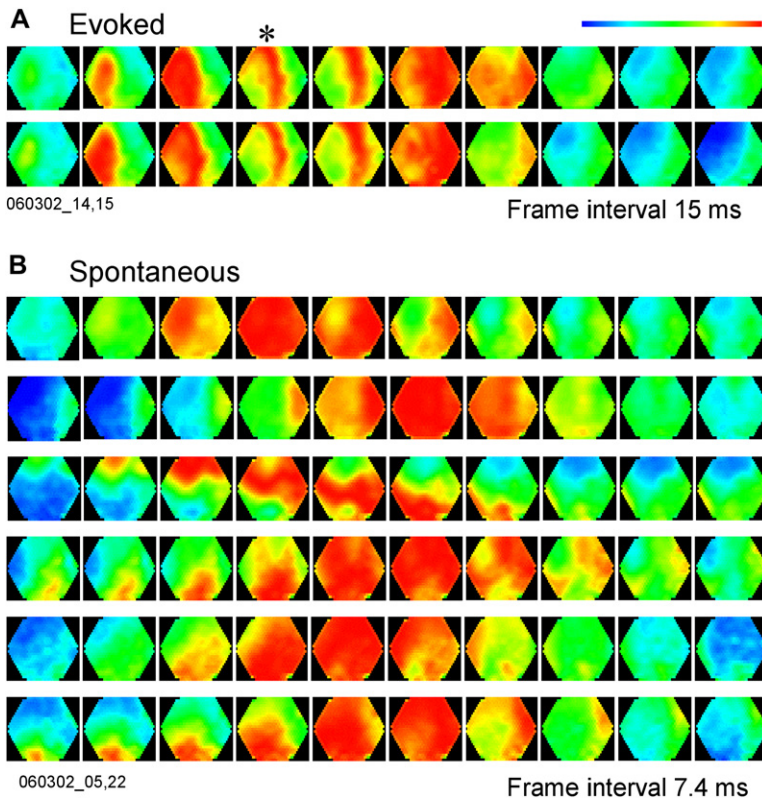


**Figure 7. Compression Only Occurs in Evoked Waves**

Images of two evoked waves (A) and six spontaneous waves (B). All images were taken from the same field of view in the same animal. The evoked response showed a clear compression at the V1/V2 border (\*) in the middle of the imaging field. Spontaneous events initiated from different locations and propagated in various directions; none had wave compression. Note that images in (A) and (B) are presented with different interframe intervals for clarity, because spontaneous events propagated faster than evoked events.

Color scale bar: the amplitude of the signal from each detector was converted to pseudo-color according to a linear color scale; red represents the peak and blue represents the baseline.

a reflected wave (Figure 7A). In contrast, the six spontaneous events all initiated from different locations and propagated across the cortex with various directions (Figure 7B). Compression and reflection were not observed during these spontaneous waves.

To further elucidate the difference between evoked and spontaneous waves, we examined a large number of spontaneous and evoked events. Figure 8A shows the distribution of initiation sites of 20 evoked events and 123 spontaneous events from one animal. The initiation sites of the evoked events were clustered in the V1M, while the spontaneous events started at various locations, many of which were from outside of the imaged area. Since the evoked waves underwent compression at the V1/V2 border, their overall propagating velocity might be slower than that of spontaneous waves. The velocity of 89 evoked and 354 spontaneous events in five animals was examined (Figure 8B). We recorded the peak time for a wave to reach each detector and calculated the SD of the peak time for all detectors (Figure 8B, left). A larger SD indicates either a longer delay between initiation site and other locations or a slower wave, while smaller SD indicates shorter delay or a faster wave. (This method simplifies the calculation of the velocity because propagation direction vectors can be ignored.) The distribution of SDs showed that most of the evoked events had large SDs compared with the spontaneous ones (Figure 8B, right,  $p < 0.001$ ,  $t$  test); while SDs of 80% of spontaneous events

were between 0–20 ms, 80% of evoked SDs were between 20–40 ms.

## DISCUSSION

The principal findings of this study are as follows: (1) visually evoked activity in rat visual cortex manifests as a wave propagating from V1 to other visual cortical areas. (2) The evoked wave is compressed at the border between visual areas, and a reflected wave is initiated after the compression. The compression and reflection occur robustly and reproducibly in different trials and in different animals. (3) GABAergic inhibition near the border between V1 and V2 plays a major role in the wave compression. (4) The compression and reflection occur in visually evoked waves, but not during spontaneous events, suggesting that the compression/reflection pattern is governed by a mechanism associated with visual processing.

Studies on visual processing have emphasized the receptive fields of individual neurons and the input-output relationship at the single-cell level. Spatiotemporal dynamics due to interactions in large networks, while important to the integration of information at the system level, are much less understood. In this report, we have observed complex and highly reproducible wave patterns, which imply that an internal mechanism organizes the activity at population level. To our knowledge, such intriguing patterns have not been reported in the previous studies of

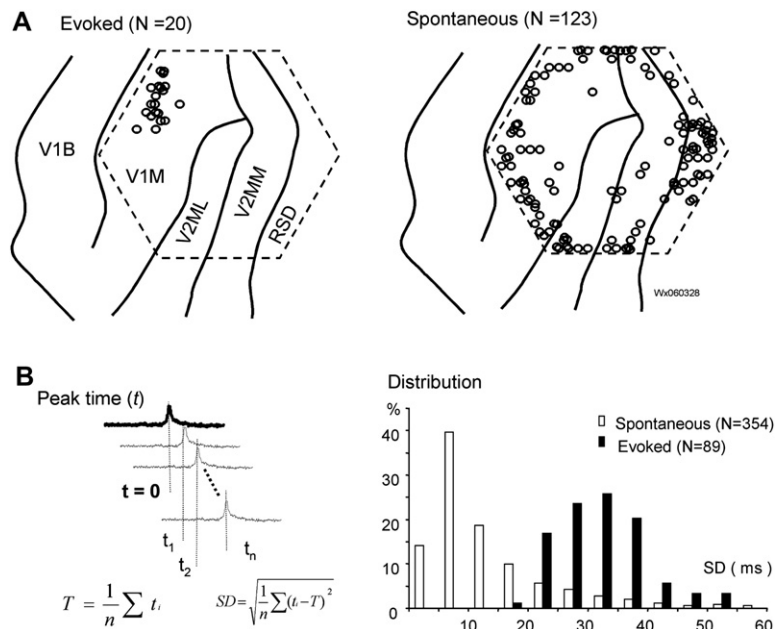


**Figure 8. Comparison of Evoked and Spontaneous Events**

(A) Initiation sites of spontaneous and evoked events from one animal. The hexagons mark the imaging field. (Left) The initiation sites of 20 evoked events; all were in area V1M. (Right) The initiation sites of 123 spontaneous events are distributed in various locations. (When a spontaneous event was initiated outside of the field of view, its initiation site was marked as the center of the wavefront when it entered the field of view.)

(B) Propagating velocity of the waves. (Left) The peak time ( $t$ , the time of peak response at that detector) was measured for all detectors (when multiple wave peaks occurred, only the first peak was counted). Bold trace: initiation site,  $t = 0$ . Standard deviation (SD, bottom equations) of the peak time is used to quantify the distribution of propagation velocity over the imaging field. (Right) Distribution of SDs in evoked and spontaneous events (443 events in five animals). The spontaneous events (white bars) have smaller SDs on average (80% between 0 and 20 ms), while the evoked events (black bars) have greater SDs on average (80% are ~20–40 ms).

cortical waves. This is probably because the wave compression/reflection pattern is not time-locked to the onset of stimuli and may be blurred when averaging multiple trials. Thus, visualizing waves in single trials using blue VSDs (Shoham et al., 1999) and a high dynamic range imaging apparatus (Wu and Cohen, 1993; Lippert et al., 2007) is essential for our findings.

### Propagating Waves in Sensory Cortices

In mammalian sensory cortex, sensory-evoked propagating waves were found in previous imaging studies using blue dyes (Derdikman et al., 2003; Petersen et al., 2003a; Roland et al., 2006). During these waves, neurons in layers II–III depolarize for a few millivolts above the resting potential (Petersen et al., 2003b), and thus the firing probability is modulated. Multiple peaks in VSD signal (e.g., Figure 1, traces 1 and 2) during the primary and reflected waves suggest biphasic responses in the spiking of individual neurons (see Figure 4 of Roland et al., 2006).

As a common feature, sensory-evoked waves robustly initiated from the location of cortical afferents and propagated over a large area. Due to the propagation, a time delay is spatially distributed over the cortical area as determined by the propagating velocity. On a population scale, such delayed activation is different from the synchrony on a millisecond scale between active neurons. Wave compression/reflection observed in this report suggests an even larger time delay, in that the depolarization in V2 is ~30 ms after V1 is activated (Figure 5C). The reflected wave, in contrast, would allow V1 and V2 to be depolarized together within 10 ms following the compression. This distinct temporal pattern provides a mechanism

for simultaneously depolarizing neurons in several visual areas. Neurons in two different visual areas may simultaneously increase their firing probability during the wave, within a particular period after receiving a visual stimulus, thus facilitating the information exchange between these areas.

Feedback waves traveling from areas 21 and 19 toward area 18 and 17 were recently reported by VSD imaging in ferrets (Roland et al., 2006). While marked differences in latency and propagating velocity were seen between their data and ours, in general, both forward and backward waves were observed, thus suggesting that propagating waves are common phenomena during visual processing.

### Stereotypical Pattern during Visually Evoked Activity

Compression/reflection was observed in every animal, suggesting that there is a stereotypical pattern of cortical activity for processing visual information. This pattern is likely to be governed by an internal mechanism that is not activated during spontaneous events. Propagating waves are known to change velocity, direction, or both due to dynamic interactions with other waves. For example, in brain slices, the collision of two waves propagating toward each other results in annihilation (Wu et al., 1999) or the formation of spiral waves (Huang et al., 2004; Schiff et al., 2007). Reflection has also been frequently observed in brain slices (Bao and Wu, 2003). However, wave-to-wave interactions in brain slices occurred at various locations with uncertain wave patterns (Huang et al., 2004). Such interactions are dynamic and different from the wave compression/reflection reported here, because the latter occurred at a fixed location and had a similar pattern from trial to trial (Figure 2).

Wave compression is a result of sudden reduction of propagating velocity of the leading edge of the wave near the V1/V2 border (Figure 5C). We consider two possible mechanisms underlying the abrupt slowdown of the leading edge: one is a reduction in the horizontal connections near the V1/V2 border, and the second is an increase in the local circuit inhibition. Abundant horizontal connections exist between the pyramidal neurons in layers II–III of visual cortex (Gilbert and Wiesel, 1979; Rockland and Lund, 1982, 1983; Livingstone and Hubel, 1984; Martin and Whitteridge, 1984; Gilbert and Wiesel, 1989), which are thought to mediate the subthreshold activation over a large area (Das and Gilbert, 1995; Toth et al., 1996). Computational models suggest that reflected waves can also occur when a wave runs into an area with decreased excitatory interactions (Ermentrout and Rinzel, 1996). However, changes of horizontal excitatory connections near the V1/V2 border itself cannot explain the wave compression, because spontaneous waves do not slow down at the V1/V2 border (Figure 7). Dynamic increase of GABA<sub>A</sub> inhibition during the evoked activity offers another mechanism. Inhibition in local cortical circuits is known to be important for controlling propagation velocity (Traub et al., 1987; Chervin et al., 1988; Miles et al., 1988; Chagnac-Amitai and Connors, 1989; Wadman and Gutnick, 1993; Golomb and Amitai, 1997; Laaris et al., 2000; Wu et al., 2001; Golomb and Ermentrout, 2002). Indeed, we found that bicuculline completely eliminated the compression at the V1/V2 border (Figure 6), suggesting that GABA<sub>A</sub> inhibition provides a mechanism for the wave compression. Such inhibition is dynamic and temporary because it is exclusively related to visually evoked waves. Interictal-like spikes occur in visual cortex when 10%–20% of GABA<sub>A</sub> inhibition is reduced (Chagnac-Amitai and Connors, 1989). Wave compression can be disrupted below the threshold of interictal-like spikes, suggesting that wave compression requires a delicate balance of GABAergic inhibition.

From a computational perspective, cortical neuronal populations may be viewed as loosely coupled oscillators (Grannan and Kleinfeld, 1993). A visual stimulus may increase the interactions and change phase shift among the oscillators. When the stimulus reaches threshold, the magnitude of the interactions will be high enough to initiate the primary wave. The velocity of the propagation of the wave may be determined by the phase shift among the neuronal oscillators (Ermentrout and Kleinfeld, 2001). Our results suggest that GABAergic inhibition also increased during evoked events, causing wave compression at the border between visual areas. Apparently, spontaneous waves are sustained by a different process; cortical neurons may receive nonspecific and synchronized input from subcortical structures (Steriade, 1997), resulting in a small phase shift and a fast overall propagation velocity.

We have observed the same propagation pattern when the stimulus was drifting at various orientations. This may be due to the lack of orientation columns in rodent visual

cortex, with cells responding to different stimulus orientations mixed in the V1 area (Girman et al., 1999; Ohki et al., 2005; Van Hooser et al., 2005; Yoshimura et al., 2005). The intercolumnar projections in layers II–III and light scattering in cortical tissue are potential factors that might blur the boundary of the columnar structures. However, stimuli presented at different locations in the visual field did affect the shape and location of the compression band (Figures S3A and S3B), suggesting interactions between propagation waves and cortical columnar structures. We speculate that in species with well-developed orientation columns, the fine structure of the initiation of the wave may vary when the orientation of the visual stimulus changes.

In conclusion, we have observed a stereotypical pattern of wave compression and reflection during visually evoked cortical activity. This pattern occurs robustly during a variety of visual stimuli, but not during spontaneous events. Such patterns may provide a mechanism to simultaneously depolarize a large population of neurons across two visual areas, and may have important implications for visual processing.

## EXPERIMENTAL PROCEDURES

### Surgical Procedures

Adult Long-Evans rats (250–400 g,  $n = 36$ ) were used in the experiments. Surgical procedures were approved by Georgetown University Animal Care and Use Committee, strictly following NIH recommendations and guidelines.

Before surgery, the animal was given an intraperitoneal (i.p.) injection of atropine (60  $\mu\text{g}/\text{kg}$ ). Anesthesia was induced with 4% isoflurane in air. After a tracheostomy tube was inserted, the animal was connected to a small animal respirator (Harvard Apparatus) and the concentration of isoflurane was reduced to 2.5% in pure oxygen for surgery and 1.5%–2.0% throughout the imaging experiment. The respiratory rate (60–100 c/min) and volume (2–3 ml) were adjusted such that the inspiratory pressure was between 5 and 10 mm H<sub>2</sub>O and the end-tidal (ET) CO<sub>2</sub> was 25–35 mm Hg (3.3%–4.6%). The body temperature of the anesthetized animals was maintained at 37°C with a regulated heating pad. A cranial window (5 × 5 mm<sup>2</sup>) was drilled over the visual cortex of the left hemisphere (bregma –4 to –9 mm, lateral 0.5–5.5 mm). The bone was carefully separated from the dura and great care was taken to avoid irritating the dura and the cortex underneath by touching or excessive pressure. Irritated dura or cortex often led to poor staining, and thus careful craniotomy was important for successful staining. In some experiments, dexamethasone sulfate (1 mg/kg i.p.) was given a few hours prior to the surgery to reduce the inflammatory response of the dura.

### Dye Staining

The cortex was stained through the dura. Leaving dura intact significantly reduces the movement artifact during optical recording (London et al., 1989). In order to increase the dural permeability to the dye, we dried the dura with gentle airflow before staining. The VSD RH-1691 or RH-1838 (Optical Imaging, [www.opt-imaging.com](http://www.opt-imaging.com)) was dissolved in Ringer's solution (1–2 mg/ml), and ~200  $\mu\text{l}$  dye solution was used for staining an area 5 mm in diameter. During staining, the dye solution was continuously circulated by a perfusion pump (London et al., 1989). The pump drew a small amount (~100  $\mu\text{l}$ ) of the dye solution from the top of the dura, held it for half a second, and then released the drop back to the pool. Using circulation greatly improved the staining quality. After staining for 90 min, the cortex was washed with dye-free Ringer's solution for ~30 min. Our method provided a good

staining over cortical layers I–III (Figure S6), similar to that achieved when staining without dura (Kleinfeld and Delaney, 1996; Ferezou et al., 2006).

### Optical Imaging

The cortex was imaged with a 5 × microscope (Kleinfeld et al., 1994) with a field of view approximately 4 mm in diameter. Light from a tungsten filament lamp (12V, 100W, Zeiss) was filtered by a  $630 \pm 15$  nm interference filter and then reflected down onto the cortex via a 655 nm dichroic mirror (Chroma Technology). Köhler illumination was achieved through the microscope. The cortex was exposed to the light only during recording trials. Dye fluorescence was filtered with a 695 nm long-pass filter and projected onto the fiber optic aperture of a 464 channel photodiode array (WuTech Instruments). Each channel (pixel) of the array received light from a cortical area of 160  $\mu\text{m}$  in diameter. The photocurrent from each channel was individually amplified with a two-stage amplifier system (Wu and Cohen, 1993). At the output of the second stage amplifier, a signal of  $10^{-3}$  spanned a range of 6 bits when digitized with a 12 bit A/D converter at 1.6 kHz.

Local EEG, ECG, tracheal respiratory pressure, and sensor signal monitoring the visual stimulation were digitized simultaneously with the optical channels. Local EEG was recorded with a silver ball electrode placed at the corner of the imaging field, amplified 1000 times, and filtered between 0.2 and 400 Hz. ECG and tracheal pressure were used for removing pulsation and respiration artifacts offline.

### Subtracting Brain Pulsation Artifact

Pulsation and respiration artifacts were time-locked to the ECG and tracheal pressure, and an algorithm was used to separate the artifacts from the signal. The algorithm was modified from our previous methods (Ma et al., 2004). Briefly, an “averaged pulsation artifact” was obtained for each optical detector. During each 5 s recording trial, there were  $\sim 30$  heartbeats. Since neuronal activity was not time-locked to the ECG, in the averaged pulsation artifact, the signal would be reduced  $\sim 30$  fold. Therefore, ECG-triggered subtraction removes the components time-locked to the ECG, but has little effect on the signal. The algorithm was implemented in Matlab (Mathworks, Natick, MA). We used NeuroPlex (RedshirtImaging, Decatur, GA) to record and view data during experiments and Matlab for data analysis and making figures.

### Sensitivity of Optical Imaging

In order to verify the sensitivity of VSD recording, we simultaneously recorded the optical signal and local field potentials from the same location in visual cortex (Figure S1). Under isoflurane anesthesia, both spontaneous and evoked events in the local field potential were also seen in the VSD signals (Figures S1A and S1B). Note that almost every peak in the local EEG also occurs in the optical recordings, demonstrating that the sensitivity of our optical recording is comparable to that of local EEG recordings. This sensitivity is essential for visualizing wave compression/reflection in single trials without averaging. However, the waveforms of the EEG and optical recordings are not exactly the same, probably because the local EEG electrode picked up signals from strong current sources in deep cortical layers or subcortical structures, while the VSD signal was localized to the neurons in cortical layers I–III under each optical detector.

### Stimulation

Visual stimulation patterns were generated by programs written in Visual C++. The patterns were displayed by a screen projector, projecting to a screen of 10 × 7 inches. The resolution of the projector was 1024 × 768 with a refresh rate of 60 Hz. The screen was placed approximately 20 cm in front of the animal's contralateral eye (Figure S2). The visual stimulus presented to the contralateral eye cannot be seen by the ipsilateral eye, and so the ipsilateral eye was not covered in the most of the experiments. A sinusoidal grating (0.02–0.3 cycles/degree, 50w × 38h degrees of viewing angle) was constantly presented to the

contralateral eye. The stimulation is the drifting of the grating. The stimulation duration was  $\sim 500$ –2000 ms and the velocity of the drifting was 30–200 degree/s. Visual stimulation was monitored by a photosensor attached to the corner of the screen. The output of the sensor was digitized simultaneously with the imaging data.

### Data Analysis and Pseudocolor Images

Data analysis was done with scripts written with Matlab (Mathworks). The pseudocolor images and movies were generated from the fractional changes of the fluorescent light on a linear color scale. Briefly, during data acquisition, the resting fluorescent light on each detector was removed by the amplifier hardware and the fractional changes in the fluorescence were amplified and digitized. In data analysis the fractional change in light on each detector was normalized between prestimulus baseline and the peak of the primary wave. The normalized value was assigned to colors (red = 1 to blue = 0) according to a linear pseudocolor scale (Grinvald et al., 1982; Jin et al., 2002; Ma et al., 2004).

### Supplemental Data

The Supplemental Data for this article can be found online at <http://www.neuron.org/cgi/content/full/55/1/119/DC1>.

### ACKNOWLEDGMENTS

We thank Drs. L.B. Cohen, G.B. Ermentrout, S.J. Schiff, S. Vicini, B. Tian, and E. Galloway for helpful discussions. This work was supported by NIH grant NS36447 (J.-Y.W.), the American Epilepsy Society, and the Lennox Trust Fund (X.H.).

Received: January 24, 2007

Revised: May 7, 2007

Accepted: June 11, 2007

Published: July 5, 2007

### REFERENCES

- Angelucci, A., Levitt, J.B., Walton, E.J., Hupe, J.M., Bullier, J., and Lund, J.S. (2002). Circuits for local and global signal integration in primary visual cortex. *J. Neurosci.* 22, 8633–8646.
- Arieli, A., Shoham, D., Hildesheim, R., and Grinvald, A. (1995). Coherent spatiotemporal patterns of ongoing activity revealed by real-time optical imaging coupled with single-unit recording in the cat visual cortex. *J. Neurophysiol.* 73, 2072–2093.
- Bao, W., and Wu, J.Y. (2003). Propagating wave and irregular dynamics: spatiotemporal patterns of cholinergic theta oscillations in neocortex in vitro. *J. Neurophysiol.* 90, 333–341.
- Chagnac-Amitai, Y., and Connors, B.W. (1989). Horizontal spread of synchronized activity in neocortex and its control by GABA-mediated inhibition. *J. Neurophysiol.* 61, 747–758.
- Chen, Y., Geisler, W.S., and Seidemann, E. (2006). Optimal decoding of correlated neural population responses in the primate visual cortex. *Nat. Neurosci.* 9, 1412–1420.
- Chervin, R.D., Pierce, P.A., and Connors, B.W. (1988). Periodicity and directionality in the propagation of epileptiform discharges across neocortex. *J. Neurophysiol.* 60, 1695–1713.
- Civillico, E.F., and Contreras, D. (2006). Integration of evoked responses in supragranular cortex studied with optical recordings in vivo. *J. Neurophysiol.* 96, 336–351.
- Das, A., and Gilbert, C.D. (1995). Long-range horizontal connections and their role in cortical reorganization revealed by optical recording of cat primary visual cortex. *Nature* 375, 780–784.
- Delaney, K.R., Gelperin, A., Fee, M.S., Flores, J.A., Gervais, R., Tank, D.W., and Kleinfeld, D. (1994). Waves and stimulus-modulated

- dynamics in an oscillating olfactory network. *Proc. Natl. Acad. Sci. USA* 91, 669–673.
- Derdikman, D., Hildesheim, R., Ahissar, E., Arieli, A., and Grinvald, A. (2003). Imaging spatiotemporal dynamics of surround inhibition in the barrels somatosensory cortex. *J. Neurosci.* 23, 3100–3105.
- Ermentrout, G.B., and Kleinfeld, D. (2001). Traveling electrical waves in cortex: insights from phase dynamics and speculation on a computational role. *Neuron* 29, 33–44.
- Ermentrout, G.B., and Rinzel, J. (1996). Reflected waves in an inhomogeneous excitable medium. *SIAM J. Appl. Math.* 56, 1107–1128.
- Ferezou, I., Bolea, S., and Petersen, C.C. (2006). Visualizing the cortical representation of whisker touch: voltage-sensitive dye imaging in freely moving mice. *Neuron* 50, 617–629.
- Freeman, W.J., and Barrie, J.M. (2000). Analysis of spatial patterns of phase in neocortical gamma EEGs in rabbit. *J. Neurophysiol.* 84, 1266–1278.
- Gilbert, C.D., and Wiesel, T.N. (1979). Morphology and intracortical projections of functionally characterized neurones in the cat visual cortex. *Nature* 280, 120–125.
- Gilbert, C.D., and Wiesel, T.N. (1989). Columnar specificity of intrinsic horizontal and corticocortical connections in cat visual cortex. *J. Neurosci.* 9, 2432–2442.
- Girman, S.V., Sauve, Y., and Lund, R.D. (1999). Receptive field properties of single neurons in rat primary visual cortex. *J. Neurophysiol.* 82, 301–311.
- Golomb, D., and Amitai, Y. (1997). Propagating neuronal discharges in neocortical slices: computational and experimental study. *J. Neurophysiol.* 78, 1199–1211.
- Golomb, D., and Ermentrout, G.B. (2002). Slow excitation supports propagation of slow pulses in networks of excitatory and inhibitory populations. *Phys. Rev. E. Stat. Nonlin. Soft Matter Phys.* 65, 061911.
- Grannan, E.R., and Kleinfeld, D. (1993). Stimulus-dependent synchronization of neuronal assemblies. *Neural Comput.* 5, 550–569.
- Grinvald, A., and Hildesheim, R. (2004). VSDI: a new era in functional imaging of cortical dynamics. *Nat. Rev. Neurosci.* 5, 874–885.
- Grinvald, A., Manker, A., and Segal, M. (1982). Visualization of the spread of electrical activity in rat hippocampal slices by voltage-sensitive optical probes. *J. Physiol.* 333, 269–291.
- Huang, X., Troy, W.C., Yang, Q., Ma, H., Laing, C.R., Schiff, S.J., and Wu, J.Y. (2004). Spiral waves in disinhibited mammalian neocortex. *J. Neurosci.* 24, 9897–9902.
- Jin, W., Zhang, R.J., and Wu, J.Y. (2002). Voltage-sensitive dye imaging of population neuronal activity in cortical tissue. *J. Neurosci. Methods* 115, 13–27.
- Kennedy, H., and Bullier, J. (1985). A double-labeling investigation of the afferent connectivity to cortical areas V1 and V2 of the macaque monkey. *J. Neurosci.* 5, 2815–2830.
- Kleinfeld, D., and Delaney, K.R. (1996). Distributed representation of vibrissa movement in the upper layers of somatosensory cortex revealed with voltage-sensitive dyes. *J. Comp. Neurol.* 375, 89–108.
- Kleinfeld, D., Delaney, K.R., Fee, M.S., Flores, J.A., Tank, D.W., and Gelperin, A. (1994). Dynamics of propagating waves in the olfactory network of a terrestrial mollusk: an electrical and optical study. *J. Neurophysiol.* 72, 1402–1419.
- Laaris, N., Carlson, G.C., and Keller, A. (2000). Thalamic-evoked synaptic interactions in barrel cortex revealed by optical imaging. *J. Neurosci.* 20, 1529–1537.
- Lam, Y.W., Cohen, L.B., Wachowiak, M., and Zochowski, M.R. (2000). Odors elicit three different oscillations in the turtle olfactory bulb. *J. Neurosci.* 20, 749–762.
- Lam, Y.W., Cohen, L.B., and Zochowski, M.R. (2003). Odorant specificity of three oscillations and the DC signal in the turtle olfactory bulb. *Eur. J. Neurosci.* 17, 436–446.
- Lippert, M.T., Takagaki, K., Xu, W., Huang, X., and Wu, J.Y. (2007). Methods for voltage-sensitive dye imaging of rat cortical activity with high signal-to-noise ratio. *J. Neurophysiol.*, in press. Published online May 9, 2007. 10.1152/jn.01169.2006.
- Livingstone, M.S., and Hubel, D.H. (1984). Specificity of intrinsic connections in primate primary visual cortex. *J. Neurosci.* 4, 2830–2835.
- Livingstone, M.S., and Hubel, D.H. (1987). Connections between layer 4B of area 17 and the thick cytochrome oxidase stripes of area 18 in the squirrel monkey. *J. Neurosci.* 7, 3371–3377.
- Livingstone, M.S., and Hubel, D.H. (1988). Segregation of form, color, movement, and depth: anatomy, physiology, and perception. *Science* 240, 740–749.
- London, J.A., Cohen, L.B., and Wu, J.Y. (1989). Optical recordings of the cortical response to whisker stimulation before and after the addition of an epileptogenic agent. *J. Neurosci.* 9, 2182–2190.
- Ma, H.T., Wu, C.H., and Wu, J.Y. (2004). Initiation of spontaneous epileptiform events in the rat neocortex in vivo. *J. Neurophysiol.* 91, 934–945.
- Martin, K.A., and Whitteridge, D. (1984). Form, function and intracortical projections of spiny neurones in the striate visual cortex of the cat. *J. Physiol.* 353, 463–504.
- Miles, R., Traub, R.D., and Wong, R.K. (1988). Spread of synchronous firing in longitudinal slices from the CA3 region of the hippocampus. *J. Neurophysiol.* 60, 1481–1496.
- Ohki, K., Chung, S., Ch'ng, Y.H., Kara, P., and Reid, R.C. (2005). Functional imaging with cellular resolution reveals precise micro-architecture in visual cortex. *Nature* 433, 597–603.
- Olavarria, J.F., and Hiroi, R. (2003). Retinal influences specify corticocortical maps by postnatal day six in rats and mice. *J. Comp. Neurol.* 459, 156–172.
- Paxinos, G., and Watson, C. (2005). *The Rat Brain in Stereotaxic Coordinates*, Fifth Edition (New York: Elsevier Academic Press).
- Petersen, C.C., Grinvald, A., and Sakmann, B. (2003a). Spatiotemporal dynamics of sensory responses in layer 2/3 of rat barrel cortex measured in vivo by voltage-sensitive dye imaging combined with whole-cell voltage recordings and neuron reconstructions. *J. Neurosci.* 23, 1298–1309.
- Petersen, C.C., Hahn, T.T., Mehta, M., Grinvald, A., and Sakmann, B. (2003b). Interaction of sensory responses with spontaneous depolarization in layer 2/3 barrel cortex. *Proc. Natl. Acad. Sci. USA* 100, 13638–13643.
- Prechtl, J.C., Cohen, L.B., Pesaran, B., Mitra, P.P., and Kleinfeld, D. (1997). Visual stimuli induce waves of electrical activity in turtle cortex. *Proc. Natl. Acad. Sci. USA* 94, 7621–7626.
- Prechtl, J.C., Bullock, T.H., and Kleinfeld, D. (2000). Direct evidence for local oscillatory current sources and intracortical phase gradients in turtle visual cortex. *Proc. Natl. Acad. Sci. USA* 97, 877–882.
- Rockland, K.S., and Lund, J.S. (1982). Widespread periodic intrinsic connections in the tree shrew visual cortex. *Science* 215, 1532–1534.
- Rockland, K.S., and Lund, J.S. (1983). Intrinsic laminar lattice connections in primate visual cortex. *J. Comp. Neurol.* 216, 303–318.
- Rockland, K.S., and Pandya, D.N. (1981). Cortical connections of the occipital lobe in the rhesus monkey: interconnections between areas 17, 18, 19 and the superior temporal sulcus. *Brain Res.* 212, 249–270.
- Roland, P.E., Hanazawa, A., Undeman, C., Eriksson, D., Tompa, T., Nakamura, H., Valentiniene, S., and Ahmed, B. (2006). Cortical feedback depolarization waves: A mechanism of top-down influence on early visual areas. *Proc. Natl. Acad. Sci. USA* 103, 12586–12591.

- Rubino, D., Robbins, K.A., and Hatsopoulos, N.G. (2006). Propagating waves mediate information transfer in the motor cortex. *Nat. Neurosci.* 9, 1549–1557.
- Schiff, S.J., Huang, X., and Wu, J.Y. (2007). Dynamical evolution of spatiotemporal patterns in mammalian middle cortex. *Phys. Rev. Lett.* 98, 178102.
- Senseman, D.M., and Robbins, K.A. (1999). Modal behavior of cortical neural networks during visual processing. *J. Neurosci.* 19, RC3.
- Shmuel, A., Korman, M., Sterkin, A., Harel, M., Ullman, S., Malach, R., and Grinvald, A. (2005). Retinotopic axis specificity and selective clustering of feedback projections from V2 to V1 in the owl monkey. *J. Neurosci.* 25, 2117–2131.
- Shoham, D., Glaser, D.E., Arieli, A., Kenet, T., Wijnbergen, C., Toledo, Y., Hildesheim, R., and Grinvald, A. (1999). Imaging cortical dynamics at high spatial and temporal resolution with novel blue voltage-sensitive dyes. *Neuron* 24, 791–802.
- Sincich, L.C., and Horton, J.C. (2002a). Pale cytochrome oxidase stripes in V2 receive the richest projection from macaque striate cortex. *J. Comp. Neurol.* 447, 18–33.
- Sincich, L.C., and Horton, J.C. (2002b). Divided by cytochrome oxidase: a map of the projections from V1 to V2 in macaques. *Science* 295, 1734–1737.
- Sincich, L.C., and Horton, J.C. (2003). Independent projection streams from macaque striate cortex to the second visual area and middle temporal area. *J. Neurosci.* 23, 5684–5692.
- Steriade, M. (1997). Synchronized activities of coupled oscillators in the cerebral cortex and thalamus at different levels of vigilance. *Cereb. Cortex* 7, 583–604.
- Toth, L.J., Rao, S.C., Kim, D.S., Somers, D., and Sur, M. (1996). Sub-threshold facilitation and suppression in primary visual cortex revealed by intrinsic signal imaging. *Proc. Natl. Acad. Sci. USA* 93, 9869–9874.
- Traub, R.D., Knowles, W.D., Miles, R., and Wong, R.K. (1987). Models of the cellular mechanism underlying propagation of epileptiform activity in the CA2–CA3 region of the hippocampal slice. *Neuroscience* 27, 457–470.
- Van Hooser, S.D., Heimel, J.A., Chung, S., Nelson, S.B., and Toth, L.J. (2005). Orientation selectivity without orientation maps in visual cortex of a highly visual mammal. *J. Neurosci.* 25, 19–28.
- Wadman, W.J., and Gutnick, M.J. (1993). Non-uniform propagation of epileptiform discharge in brain slices of rat neocortex. *Neuroscience* 52, 255–262.
- Wu, J.Y., and Cohen, L.B. (1993). Fast multisite optical measurement of membrane potential. In *Biological Techniques: Fluorescent and Luminescent Probes for Biological Activity*, W.T. Mason, ed. (New York: Academic press), pp. 389–404.
- Wu, J.Y., Guan, L., and Tsau, Y. (1999). Propagating activation during oscillations and evoked responses in neocortical slices. *J. Neurosci.* 19, 5005–5015.
- Wu, J.Y., Guan, L., Bai, L., and Yang, Q. (2001). Spatiotemporal properties of an evoked population activity in rat sensory cortical slices. *J. Neurophysiol.* 86, 2461–2474.
- Yoshimura, Y., Dantzker, J.L., and Callaway, E.M. (2005). Excitatory cortical neurons form fine-scale functional networks. *Nature* 433, 868–873.